LUNAR POLAR WATER ICE: A TERRAIN CLASSIFICATION SYSTEM AND OPTIMAL SITES FOR MOON EXPLORATION. Cameron G. Moye[1,2] and Pascal Lee[2,3,4], [1]University of Maryland, College Park, MD, cameron.moye@outlook.com; [2]SETI Institute, [3]Mars Institute, [4]NASA Ames Research Center.

Summary: We classify terrains at the lunar poles on the basis of 3 key considerations: a) detection or not of H_2O ice within the top 1 m of the regolith, b) site located inside or outside Permanently Shadowed Regions (PSRs), and c) thermodynamic stability of H_2O ice in the shallow subsurface allowed or not by models. Sites presenting clear H_2O ice signatures located *outside* PSRs might offer optimal targets for early exploration.

Introduction: H_2O ice is potentially present at the lunar poles, to first order in association with their PSRs [1,2]. This water is of considerable interest for understanding the history and distribution of volatiles in the solar system, the role of volatiles in the evolution of the Earth-Moon system, and its potential as a resource for future human space exploration [3]. However, the relationship between areas in which H_2O ice presence has been inferred and the PSRs is not straightforward. Some PSRs are associated with detected concentrations of water-equivalent hydrogen (WEH), but some PSRs are not. Conversely, there are areas at the lunar poles where H is detected *outside* of the PSRs. Because WEH estimates are based on neutron spectrometry which integrates neutron counts within the top 1 m of the regolith, a key factor to consider is whether or not physical conditions might allow H_2O ice to be stable in the subsurface. Some areas outside of PSRs are frequently shadowed and cold enough to allow H_2O ice to be stable within the top few meters, were it present.

To describe more fully the distribution of H_2O ice at the lunar poles and its dependence on these considerations, we propose a terrain classification system that distinguishes all eight permutations of the following three terrain variables: a) whether or not WEH concentrations have been detected in the terrain within the top 1m of the regolith; b) whether the terrain surface is inside or outside a PSR; c) whether or not thermodynamic stability models (combining surface illumination, topography, and regolith conductivity and diffusivity) allow H_2O ice to be stable within the top 1 m of the regolith.

Our proposed terrain classification organizes terrain units in the lunar polar regions in terms H_2O ice detections, surface environmental conditions (PSRs), and subsurface environmental conditions (subsurface thermodynamic stability). Such a classification system is helpful both for scientific studies aiming to understand the origin and 3D distribution of H_2O ice at the lunar poles, and also for characterizing operational conditions under which H_2O ice might be accessed and explored by robotic systems and humans (Artemis astronauts), for science and in-situ resource utilization (ISRU).

Classification System: Table 1 lists parameter combinations defining 8 classes of lunar polar terrains. WEH concentrations are derived from Lunar Reconnaissance Orbiter (LRO) Lunar Exploration Neutron Detector (LEND) data (10 km resolution) [4]. The thermodynamic model predicting H_2O ice stability in the top 2.5 m of the regolith is based on LRO Diviner Lunar Radiometer Experiment data (0.5 km resolution) and considers H_2O ice stable when sublimation rates are <1mm/Gyr [5]. PSR locations are derived from LRO Lunar Orbiter Laser Altimeter (LOLA) data [6].

Table 1: Lunar Polar H_2O Ice Terrain Classification

Terrain Class	H detected w/in top 1m? [4]	Located in PSR? [6]	Thermodynamic model allows H_2O ice w/in top 2.5 m? [5]
1	Yes	Yes	Yes
2	Yes	Yes	No
3	Yes	No	Yes
4	Yes	No	No
5	No	Yes	Yes
6	No	Yes	No
7	No	No	Yes
8	No	No	No

Table 1. *Classes 3+4 (yellow) are optimal for early exploration: H is detected outside PSRs. Other classes are in blue. Classes 2+6 (gray) are not real-world cases.*

Class 1. Class 1 Terrain is where H is detected where H_2O ice is most expected: inside a PSR and as allowed by the Diviner model. The PSRs inside Shackleton (D~21 km) and Cabeus (D~98 km) Craters (the latter the impact site of Lunar Crater Observation & Sensing Satellite or LCROSS) are examples of Class 1 Terrain.

Class 2 and Class 6 Terrains don't exist, as they imply that the thermodynamic model used *precludes* H_2O ice being stable inside a PSR, which it should not. These two classes are included only for completeness.

Class 3. Class 3 Terrain exhibits H concentrations within the top 1 m of the regolith and is predicted by the Diviner model to allow H_2O ice within the top 2.5 m, even though it is *outside* a PSR. An example of Class 3 Terrain: area around Shoemaker Crater (D~51 km).

Class 4. Class 4 Terrain contain H within the top 1 meter of the regolith even though it is neither a PSR nor terrain predicted to allow H_2O ice within the top 2.5 m. Such H_2O ice deposits might be relict [5]. An example of Class 4 Terrain is an area centered at 83°S, 127.3°E, ~30 km from the rim of Idel'son L Crater (D~28 km).

Classes 5 and 7. Class 5 and Class 7 Terrain are PSR and non-PSR, respectively, but both predicted by the Diviner model to allow H_2O ice to be stable within the top 2.5 m of the regolith, and both showing no H detection. Class 5 and Class 7 Terrain could include areas in which H_2O ice *might* actually be present within the top 1 m, but in concentrations below LRO LEND detection limits. Both could also allow H_2O ice to be more abundantly present, but at a depth beyond 1 m. An example of Class 5 Terrain is the PSR inside Wapowski Crater (D~11.6 km) at 82.9°S, 53.5°E. An example of a Class 7 Terrain is an area centered at 82.29°S 3.28°E, just North of Malapert Crater (D~69 km).

Class 8. Class 8 Terrain does not have H detections by LEND, is not within a PSR, and is not predicted to allow H_2O ice within the top 2.5 m of the regolith. The majority of the lunar surface may be considered Class 8.

Additional Parameters and Subclasses: The proposed classification system is expandable into more classes and subclasses, to take into account additional factors. For instance, while Classes 3 and 4 Terrain contain concentrations of WEH and are outside PSRs, illumination conditions in these non-PSR areas vary over a wide range. Given the full lunation duration of 29.5 Earth days, one could distinguish subclasses of terrains with different fractional amounts of insolation time. For longer insolation durations, the H_2O ice stability depth would generally increase, but solar powered missions might operate at lower risk in such areas.

Optimal Terrain for Early Exploration: H_2O ice deposits in the lunar polar regions do not map identically with the PSRs. Class 3 and 4 Terrains encompass the areas presenting H detections within the top 1 m of the regolith *and* are non-PSRs. Although Class 3 and 4 Terrains include areas remaining shadowed for substantial fractions of a lunation, some sites receive so much solar illumination that H_2O ice is disallowed by the Diviner model down to depths of more than ~1 m and yet LRO LEND detects H within the top 1 m. This discrepancy between observed distribution of H_2O ice and model "predictions" may be due to imperfections in the model and/or the possibility that some of the H_2O ice detected is relict, representing thermodynamic stability conditions that were different in the past [5]. Although WEH concentrations in Classes 3 and 4 are generally lower than in Class 1, Classes 3 and 4 cover substantial areas and represent a significant fraction of the H_2O ice within the top 1 m of the regolith at the lunar poles. Because non-PSRs may present exploration conditions that are less constrained (more forgiving temperature and power-wise) than PSRs, Class 3 and 4 terrain may offer optimal opportunities for early phases of near-surface H_2O ice exploration on the Moon.

Case Study: Idel'son L Crater and Vicinity. Idel'son L Crater (D~28 km), at 84.2°S,115.8°E, lies on the far side of the Moon, just behind the southern lunar limb, in an area occasionally in view of the Earth due to libration. The crater and vicinity out to 30km range present large swaths of Class 1, 3, 4 and 8 Terrains **(Fig. 1).**

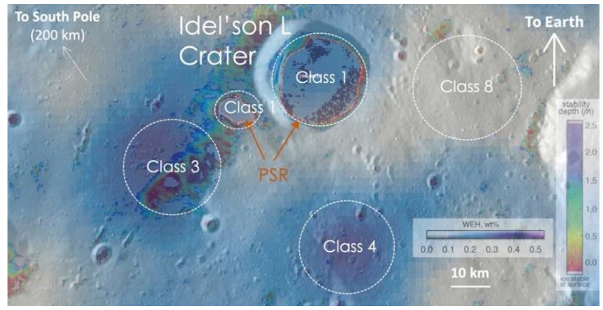

***Figure 1. Map of Idel'son L Crater and Vicinity**: Composite map of a lunar polar area presenting a variety of terrain classes (1, 3, 4, 8) within a few tens of km from each other. Here, Class 3 and 4 Terrains have WEH values of up to ~0.35 wt%, higher than within nearby PSRs.*

Conclusions: Our proposed lunar polar terrain classification system allows the complex relationship between H detection, PSRs, and modeled H_2O ice stability depth to be organized and mapped. The system may help understand the origin, age, and 3D distribution of H_2O ice at the lunar poles, and also help select optimal sites for future robotic and human exploration. Our classification system is evolvable to include additional factors such as UV/IR reflectance [7-9], radar and polarization, solar illumination duration, terrain roughness, slopes, direct-to-Earth comms visibility, etc. The spatial scale over which different terrain classes occur suggests future missions should aim to explore the lunar polar regions over ranges of tens to hundreds of kilometers in order to encounter a broad sampling of terrain classes. Mission concepts such as JPL's highly mobile Globe-Trotter soft hopper could meet such requirements [10].

Future Work: We are developing more complete terrain classification maps for both lunar poles.

Acknowledgments: C. Moye was supported by a NSF REU internship at the SETI Institute. P. Lee was supported in part by NASA via Cooperative Agreement NNX14AT27A.

References: [1] Arnold, J. (1979) *JGR*, *84*, 5659-5668. [2] Watson, K. *et al.* (1961) *JGR*, *66*, 3033-3045. [3] Anand, M. *et al.* (2012) *Planet. Space Sci.*, *74*, 42-48. [4] Sanin, A. *et al.* (2017) *Icarus*, *283*, 20-30. [5] Siegler, M. *et al.* (2016) *Nature*, *531*, 480-501. [6] Mazarico, E. *et al.* (2011) *Icarus*, *211*, 1066. [7] Hayne, P. *et al*. (2015) *Icarus*, *59*, 58-69. [8] Fisher, E. *et al*. (2017) *Icarus*, *292*, 74-85. [9] Li, S. *et al*. (2018) *PNAS*, *115*, 8907-8912. [10] Lee, P. *et al.* (2019). *NESF2019-013*.